

## The interfacial surface tension of a quark-gluon plasma fireball in a hadronic medium

R RAMANATHAN, K K GUPTA\*, AGAM K JHA and S S SINGH

Department of Physics, University of Delhi, Delhi 110 007, India

\*Department of Physics, Ramjas College, University of Delhi, Delhi 110 007, India

E-mail: dramanathan@vsnl.net

MS received 7 September 2006; revised 10 January 2007; accepted 28 February 2007

**Abstract.** We calculate the interfacial surface tension of a QGP-fireball in a hadronic medium in the Ramanathan *et al* statistical model. The constancy of the ratio of the surface tension with the cube of the critical transition temperature is in overall accordance with lattice QCD findings. It is in complete agreement with a recent MIT bag model calculation of surface tension. The velocity of sound in the QGP droplet is predicted to be in the range  $(0.27 \pm 0.02)$  times the velocity of light in vacuum and this value is independent of both the value of the transition temperature and the model parameters.

**Keywords.** Quark-gluon plasma; quark-hadron phase transition.

**PACS Nos** 25.75.Ld; 12.38.Mh; 21.65.+f

### 1. Introduction

The formation of quark-gluon plasma (QGP) droplet (fireball) is one of the most exciting possibilities in the ultra-relativistic heavy ion collision (URHIC) [1]. The physics of such an event is very complicated and to extract meaningful results from a rigorous use of quantum chromodynamics (QCD), a theory of strong interaction, to this physical system is almost intractable, though heroic efforts at lattice estimation of the problem has been going on for quite some time [2]. One way out is to replicate the approximation schemes which have served as theoretical tools in understanding equally complicated atomic and nuclear systems in atomic and nuclear physics in the context of QGP droplet formation [3,4]. This approach lays no claim to rigour or *ab-initio* ‘understanding’ of the phenomenon but lays the framework on which more rigorous structures may be built depending on the phenomenological success of the model as and when testable data emerge from ongoing experiments. There is also a general consensus among experts that the QGP-hadron phase transition is most probably a weakly first-order one, and the model calculation also lends weightage to this conclusion, as this model can fit either a first-order or weakly first-order scenario.

The central assumption in this approach is that the QGP–hadron system attains a quasi-static equilibrium enabling applicability of equilibrium statistical mechanics to the system. We are not the first to make this assumption which was pioneered by the work of Satz and collaborators [1].

The nucleation process is driven by statistical fluctuations being determined by the critical free energy difference between two phases. The Csernai–Kapusta *et al* model [3,5] uses the liquid drop model expansion for this, as given by

$$\Delta F = \frac{4\pi}{3} R^3 [P_{\text{had}}(T, \mu_B) - P_{\text{q,g}}(T, \mu_B)] + 4\pi R^2 \sigma + \tau_{\text{crit}} T \ln \left[ 1 + \left( \frac{4\pi}{3} \right) R^3 s_{\text{q,g}} \right]. \quad (1)$$

The first term represents the volume contribution, the second term is the surface contribution where  $\sigma$  is the surface tension, and the last term is the so-called shape contribution. The shape contribution is an entropy term on account of fluctuations in droplet shape which we may ignore in the lowest order approximation. The critical radius  $R_c$  can be obtained by minimising (1) with respect to the droplet radius  $R$ , which in the Linde approximation [6] is

$$R_c = \frac{2\sigma}{\Delta p} \quad \text{or} \quad \sigma = \frac{3\Delta F_c}{4\pi R_c^2}. \quad (2)$$

In the approximation scheme of Ramanathan *et al* [4], the relativistic density of states for the quarks and gluons is constructed adapting the procedures of the Thomas–Fermi construction of the electronic density of states for complex atoms and the Bethe density of states [6] for nucleons in the complex nuclei as templates.

In the next two sections we outline the Ramanathan *et al* statistical model [4] and finally apply it to compute the interfacial surface tension.

## 2. A modified Thomas–Fermi model for the QGP droplet

In a very elegant and successful statistical model of atoms of large atomic numbers, Thomas and Fermi [6] demonstrated the way to compute electronic density of states to very high order of accuracy. The Thomas–Fermi model of atom assumes the electrons to be Fermi–Dirac gas confined within a localized region by the confining electrostatic potential  $V(r)$  of the central nucleus. The potential is assumed to be varying very slowly in the region with average thermal energy  $T$  (setting the Boltzmann constant to unity) and is small compared to  $V(r)$  within the region and comparable to it near the boundary.

It is now straightforward [6] to compare the electronic density of states, assuming all states to be filled in a volume  $\nu$ . The total number of states is

$$N_e = p_{\text{max}}^3 \nu / 3\pi^2. \quad (3)$$

The maximum kinetic energy of the electron at any point in phase space should not exceed the electrostatic potential (confining) at that point and therefore

*Interfacial surface tension of a QGP fireball*

$$p_{\max}^2/2m = -V(k),$$

where  $k$  is the phase point under consideration and  $V(k)$  is the momentum transform of the coordinate potential  $V(r)$ . Therefore, the total density of states in phase space is given by

$$\int \rho_e(k) dk = [-2mV(k)]^{3/2} \nu / 3\pi^2 \quad (4)$$

or

$$\rho_e(k) = [\nu(2m)^{3/2}/2\pi^2] [-V(k)]^{1/2} \cdot \left[ -\frac{dV(k)}{dk} \right]. \quad (5)$$

In a modified ‘Thomas–Fermi’ [6] model adapted to the case of a QGP droplet, the electrons get replaced by quarks which are also fermions, and the minimum kinetic energy of the quarks at each point in phase space must exceed the confining/de-confining potential at that point, since the QGP by definition is a deconfined gas of relativistic quarks and gluons as against the non-relativistic electron of the conventional Thomas–Fermi Model. Therefore,  $p_{\min} = [-V_{\text{conf}}(k)]$  and  $p_{\max} = [-V_{\text{conf}}(\infty)]$  represents a reference energy and can be set to zero, remembering that we are dealing with a relativistic system where  $k$  refers to the corresponding quark momenta in phase space. So an expression similar to eq. (5) holds for the quark-gluon density of states, with the replacement of  $V(k)$  with a suitable QCD-induced phenomenological potential. The quark-gluon density of states is therefore

$$\int \rho_{\text{q,g}} dk = [-V_{\text{conf}}(k)]^3 \nu / 3\pi^2, \quad (6)$$

or

$$\rho_{\text{q,g}}(k) = (\nu/\pi^2) \left\{ (-V_{\text{conf}}(k))^2 \left( \frac{dV_{\text{conf}}(k)}{dk} \right) \right\}_{\text{q,g}}, \quad (7)$$

where  $\nu$  is the volume occupied by the QGP and  $k$  is the relativistic four-momentum in natural units.  $V_{\text{conf}}(k)$  could be any confining potential for quarks and gluons, but for the present we choose to work with a modified thermal potential. The main reason for this choice is our failure to obtain meaningful results with other potentials available in the literature. This potential plays the role of a mean-field potential in phase space as to the mean-field potential of the Thomas–Fermi scheme, but in a very different context – namely the QGP-hadron system.

In this adaptation of the ‘Thomas–Fermi’ idea, we only capture the spirit of the original idea for a system which is very different in detail. The primary difference between the electron–gas cloud surrounding the Thomas–Fermi nuclei and the QGP is the presence of the central potential in the former and the many-body QCD potential in the latter, apart from the thermodynamically cold nature of the former system as against the hot plasma with the hydrodynamical flows in the latter. With all these differences in the background, we can still use the Thomas–Fermi density of state (5) as a template to construct the quark density of states in a QGP with suitable parametrisation to take care of the hydrodynamical (plasma) characteristics of the QGP as we introduce in the next section.

### 3. The phenomenological inter-quark potential and the free energy

The dynamical nature of the quarks and gluons in QGP forces us to seek an inter-quark potential which can account for the bulk properties (thermodynamical) of the quarks and gluons. The ideal thing to do is to find the effective mean field QCD potential analogous to the Thomas–Fermi mean field potential for the QGP–hadron system which however is a very complicated problem. So, for the present we use the thermal mass formalism and the corresponding thermal Hamiltonian in the literature [7] leading us to the following choice for the confining/de-confining potential.

The ‘thermal–Hamiltonian’ for the QGP is [7]

$$\begin{aligned} H(k, T) &= [k^2 + m^2(T)]^{1/2} \equiv k + m^2(T)/2k \quad \text{for large } k \text{ or,} \\ H(k, T) &= k + m_0^2/2k - \{m_0^2 - m^2(T)\}/2k, \end{aligned} \quad (8)$$

where

$$m^2(T) = \gamma_{g,q} g^2(k) T^2 \quad (9)$$

with  $k$  is the quark(gluon) momentum,  $m_0$  is the dynamic rest mass of the quark,  $T$  is the temperature and  $g(k)$  is the first-order QCD running coupling constant, which for quarks with three flavors is [8]

$$g^2(k) = (4/3)(12\pi/27)\{1/\ln(1 + k^2/\Lambda^2)\}, \quad (10)$$

with the QCD parameter  $\Lambda = 150$  MeV.  $\gamma_{g,q}$  is the phenomenological parameter which we take as  $\gamma_g = 1/3$  and  $\gamma_q = 1/6$  [7]. The third term in (8) can be interpreted as an effective thermal potential for the QGP which has the form

$$V_{\text{eff}}(k) = (1/2k)\gamma_{g,q}g^2(k)T^2 - m_0^2/2k. \quad (11)$$

These numerical coefficients are like the Reynold’s number in fluid flows and take care of the deviations from linearity and other expected plasma characteristics of the QGP ‘fluid’. The main advantage of this parametrisation is that it fits nicely with lattice QCD simulations [7]. However, with the choice of (10) we have hybridised the Peshier potential with the Richardson–Cornell coupling as we had earlier found, that neither the pure Richardson–Cornell potential nor the pure Peshier potential fits our bill, and numerical evaluation of the corresponding free energies are not of the desirable form.

Since the QGP is a deconfined gas of quarks and gluons, the momentum of the particles exceeds the potential of each point in phase space, whereby

$$k_{\text{min}} = V(k_{\text{min}}) \quad \text{or} \quad k_{\text{min}} = (\gamma_{g,q} N^{1/3} T^2 \Lambda^2 / 2)^{1/4}, \quad (12)$$

where  $N = (4/3)(12\pi/27)$ . The above lower bound is valid for  $k_{\text{min}} \ll \lambda$ .

The existence of  $k_{\text{min}}$  leads to a natural low energy cut-off in the model leading to finite integrals by avoiding the infra-red divergence. It is interesting to note that  $k_{\text{min}}$  is of the same order of magnitude as  $\Lambda$  and  $T$ . This is unlike the models of earlier authors who introduced the cut-off in a rather ad-hoc fashion [9].

Thus for evaluation of density of states of the quarks we have to evaluate relation (7) after introducing potential (11) in it. The gluons are also confined in the hadrons and deconfined in the QGP, and we impose the low energy cut-off for the gluon density of states as well, and this takes care of the consistency of the treatment of both the gluon and quark sectors.

For the free energy we use the usual continuum expression for a system of non-interacting fermions (upper sign) or bosons (lower sign) at temperature  $T$ . We have

$$F_i = \mp T g_i \int dk \rho_i(k) \ln(1 \pm e^{-\sqrt{m_i^2+k^2}/T}), \quad (13)$$

where  $\rho_i(k)$  is the density of states of the particular particle,  $i$  (quarks, gluons, interface, pions etc.) being the number of states with momentum between  $k$  and  $k + dk$  in a spherically symmetric situation, and  $g_i$  is the degeneracy factor (colour and spin degeneracy) which is 6 for quarks and 8 for gluons and one each for pions and the interface. The hadronic environment can be taken as mainly made up of pions following Satz and others [9] as pions are expected to be the most copious components of the hadronised state.

Unlike the assumption of the earlier authors [9], the interfacial surface is no longer a MIT bag, and yet it has a contribution to free energy on account of the surface energy which we assume to be a scalar Weyl surface [7,10] in our approach with suitable modification to take care of the hydrodynamic effects [11] at the surface. Therefore, the interface free energy is

$$F_{\text{interface}} = \gamma T \int dk \rho_{\text{Weyl}}(k) \delta(k - T), \quad (14)$$

where  $\gamma$  is a modification sought to be introduced to take care of the plasma (hydrodynamical) nature of the droplet and is consciously chosen as

$$\gamma = \sqrt{2} \times \sqrt{(1/\gamma_g)^2 + (1/\gamma_q)^2}, \quad (15)$$

which is the inverse rms value of the flow parameter of the quarks and gluons, respectively.

The Weyl density of state is

$$\rho_{\text{Weyl}}(k) = (4\pi R^2/16\pi)k^2, \quad (16)$$

$R$  being the radius of the droplet.

Therefore,

$$F_{\text{interface}} = \frac{1}{4} R^2 T^3 \gamma. \quad (17)$$

The colour degeneracy  $g_i$  is 6 for quarks and 8 for gluons.

The pion free energy is [9]

$$F_\pi = (3T/2\pi^2)\nu \int_0^\infty k^2 dk \ln \left( 1 - e^{-\sqrt{m_\pi^2+k^2}/T} \right). \quad (18)$$

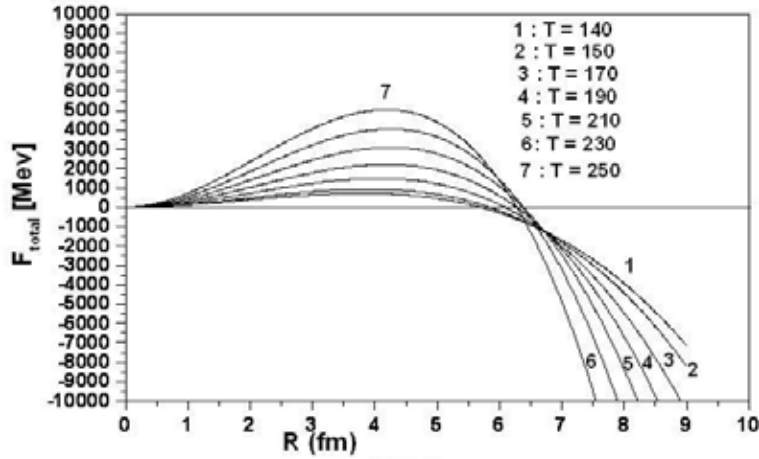


**Figure 1.**  $F_{\text{total}}$  at  $\gamma_g = 6\gamma_q$ ,  $\gamma_q = 1/6$  for various temperatures.

For quark masses we use the current (dynamic) quark masses  $m_0 = m_d = 0$  MeV and  $m_s = 150$  MeV, just as in ref. [9].

We can thus compute the total free energy  $F_{\text{total}}$  as

$$F_{\text{total}} = F_{q=u,d,s} + F_{\text{gluon}} + F_{\pi} + F_{\text{surface}}. \tag{19}$$

#### 4. Interfacial surface tension

With these ingredients we can compute the free-energy change with respect to both the droplet radius and critical temperature to get a physical picture of the fireball formation, the nucleation rate governing the droplet formation, the nature of the phase transition etc. This can be done over a whole range of flow-parameter values [4]. We exhibit only two most promising scenarios in figures 1 and 2. The above two cases are most promising as only these among other cases considered in [4] show a significant positive energy barrier essential, as we shall see later, for observable droplets to form. Further, only they exhibit formation of droplets with the observable critical droplet radius of more than a Fermi in size. Apart from these promising features, the transition temperatures in the band 150 MeV to 170 MeV, which are expected from lattice calculations also occur in these cases.

Figures 1 and 2 are the two most promising scenarios of our model which exhibit measurable droplet of radius of the order of few Fermis, and also significant barrier heights which control the nucleation rate for droplet formation. The set of parameters leading to figure 1 seems more realistic because of the bunching of the respective free energy curves at nearly equal critical droplet radius irrespective of the transition temperature unlike in figure 2. From the values of the critical free energies at the corresponding critical fireball radius that can be extracted from figures 1 and 2, we can compute the surface tension of the fireball using (2) as listed in tables 1 and 2.

Interfacial surface tension of a QGP fireball

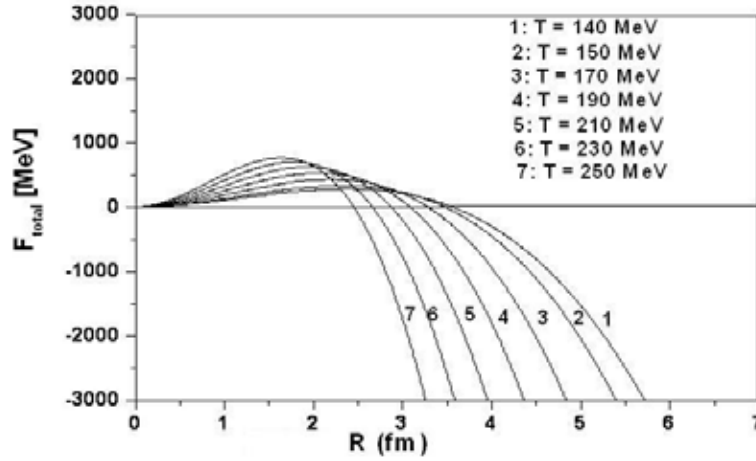


Figure 2.  $F_{\text{total}}$  at  $\gamma_g = 8\gamma_q$ ,  $\gamma_q = 1/6$  for various temperatures.

Table 1. Surface tension of the QGP droplet at  $\gamma_g = 8\gamma_q$ ,  $\gamma_q = 1/6$ .

$T_c$ (MeV)	$\Delta F_c$ (MeV)	$R_c$ (fm)	$\sigma$ (MeV/fm <sup>2</sup> )	$\sigma/T_c^3$
150	332.203	3.475	6.568	0.078
160	382.359	3.385	7.966	0.078
170	433.037	3.285	9.580	0.078
190	532.219	3.085	13.350	0.078
210	623.349	2.875	18.004	0.078
230	702.041	2.655	23.776	0.078
250	766.041	2.455	30.343	0.078

Table 2. Surface tension of the QGP droplet at  $\gamma_g = 6\gamma_q$ ,  $\gamma_q = 1/6$ .

$T_c$ (MeV)	$\Delta F_c$ (MeV)	$R_c$ (fm)	$\sigma$ (MeV/fm <sup>2</sup> )	$\sigma/T_c^3$
150	943.595	5.835	6.616	0.078
160	1197	5.965	8.031	0.078
170	1494	6.085	9.633	0.078
190	2216	6.275	13.435	0.078
210	3088	6.375	18.140	0.078
230	4059	6.375	23.844	0.078
250	5052	6.275	30.630	0.078

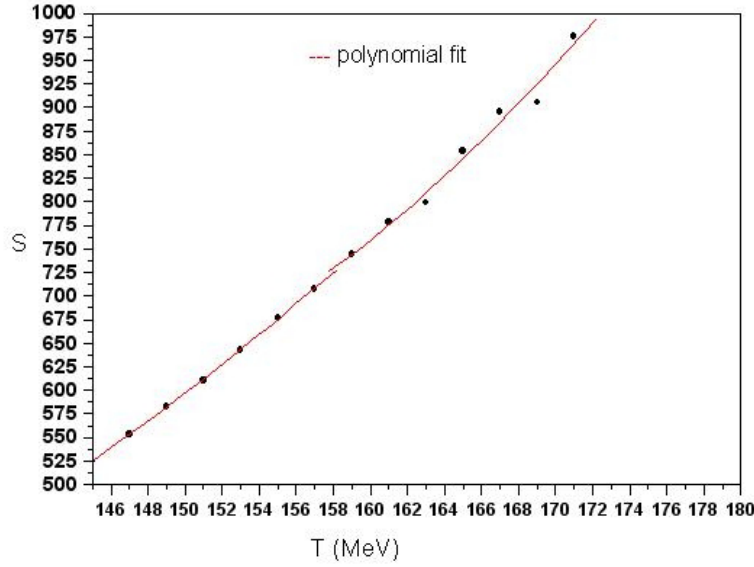


Figure 3. Variation of  $S$  with temperature  $T$  at  $\gamma_g = 6\gamma_q$ ,  $\gamma_q = 1/6$ .

It is indeed remarkable that the ratio  $\sigma/T_c^3$  is a constant irrespective of the transition temperature and the values of the model parameters.

### 5. Nature of the phase transition and the velocity of sound

Standard thermodynamics gives the following relations:

$$\text{Entropy } S = -(\partial F/\partial T), \quad (20)$$

$$\text{Specific heat } C_V = T(\partial S/\partial T)_V, \quad (21)$$

$$\text{Sound velocity } C_S^2 = S/C_V. \quad (22)$$

The behaviour of entropy  $S$  and the heat capacity  $C_V$  with temperature indicate the nature of the phase transition of the system.

After plugging the total free energy (eq. (19)) into these expressions, we evaluate these quantities for two promising scenarios of our model, the results of which are displayed in figures 3–8.

Figures 3 and 4 indicate that there exists a very weak discontinuity in the vicinity of  $T_c = 160$  MeV, in the entropy, which is a first-order thermodynamic variable. The discontinuity is just of the order of one standard deviation of the entropy variable and therefore very weak indeed. And as seen in the following temperature variation of the second-order variable  $C_V$  (figures 5 and 6), there is absolutely no discontinuity.

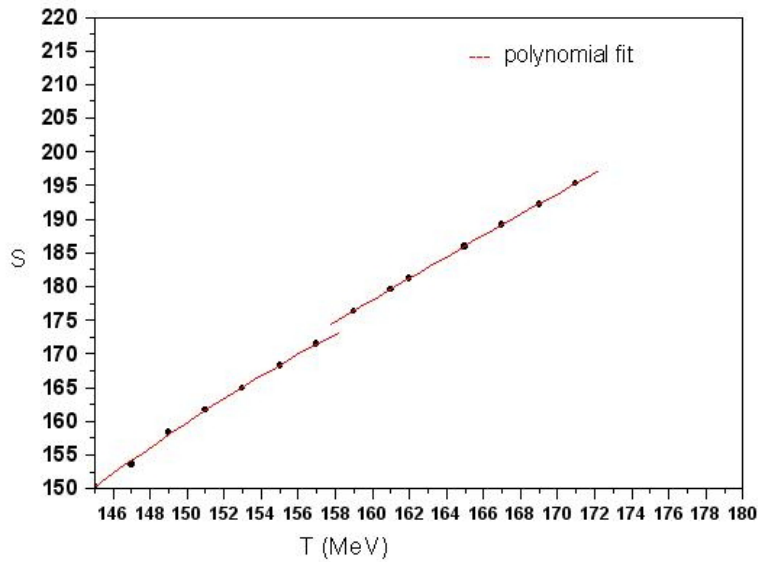


Figure 4. Variation of  $S$  with temperature  $T$  at  $\gamma_g = 8\gamma_q$ ,  $\gamma_q = 1/6$ .

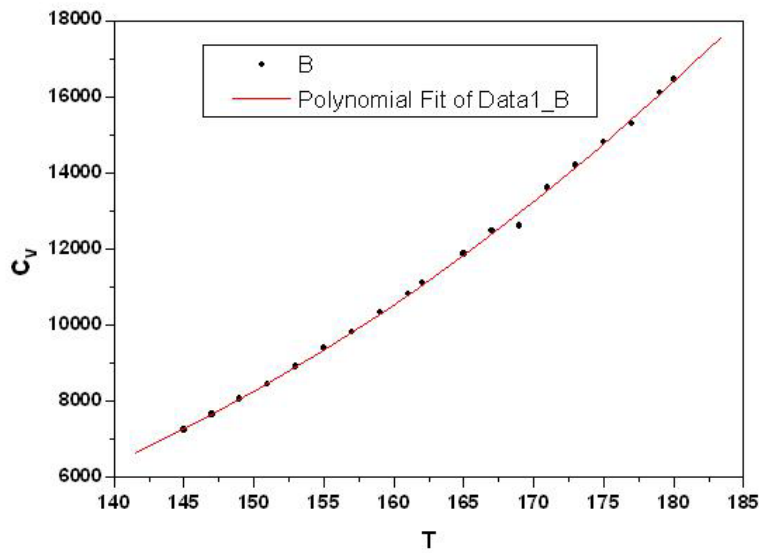
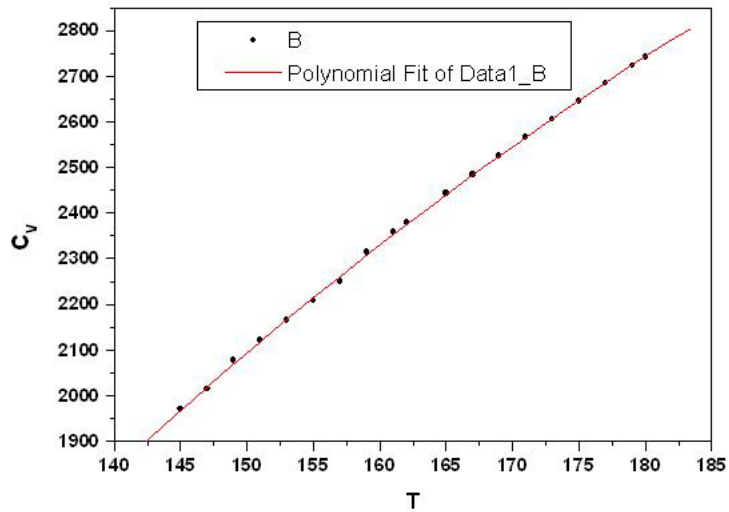
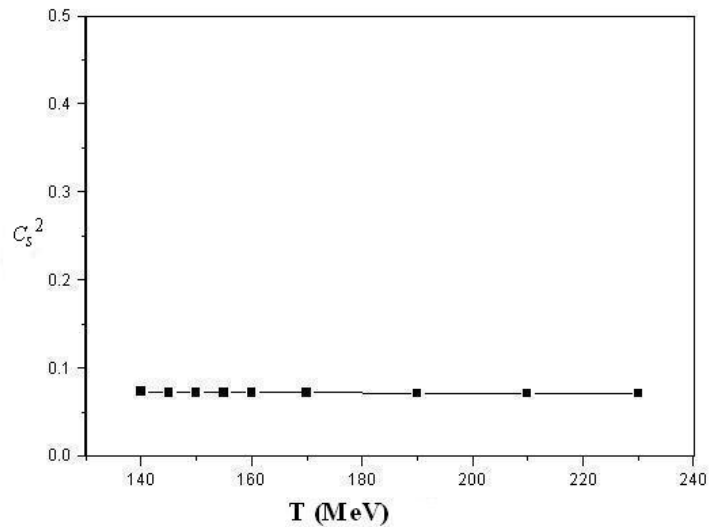


Figure 5. Variation of specific heat  $C_V$  with temperature  $T$  at  $\gamma_g = 6\gamma_q$ ,  $\gamma_q = 1/6$ .

Using the values of  $S$  and  $C_V$  from figures 3–6, we can calculate the velocity of the sound in the system using eq. (22). It is reassuring to find once again that the model predicts an almost constant value for this quantity irrespective of the transition temperature and the model parameters.



**Figure 6.** Variation of specific heat  $C_V$  with temperature  $T$  at  $\gamma_g = 8\gamma_q$ ,  $\gamma_q = 1/6$ .



**Figure 7.** Variation of velocity of sound squared  $C_s^2$  with temperature  $T$  at  $\gamma_g = 6\gamma_q$ ,  $\gamma_q = 1/6$ .

## 6. Conclusions

In tables 1 and 2 the surface tension is seen to increase with the critical temperature of the fireball, which is a beautiful demonstration of a QCD effect. As the critical temperature of the QGP droplet increases, the shear forces on the fireball surface will also increase tending to tear the surface quarks apart, consequently, bringing

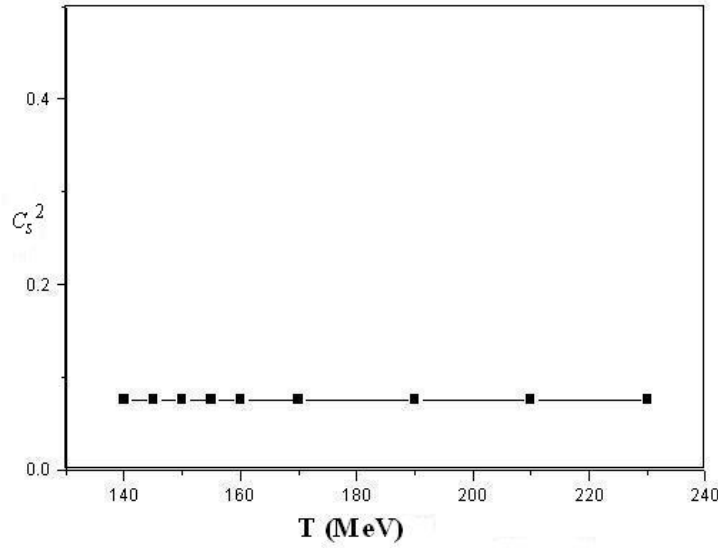


**Figure 8.** Variation of velocity of sound squared  $C_s^2$  with temperature  $T$  at  $\gamma_g = 8\gamma_q$ ,  $\gamma_q = 1/6$ .

into play the confining property of the QCD forces manifesting itself in increased surface tension, which is exactly what the calculations show. It has to be kept in mind that our model does not fix the critical temperature of transition, but only deals with all possible candidate critical temperatures out of which possibly, only one will be chosen by nature. Of course, this is not surprising as the confining feature of QCD has been incorporated in (4), but it is nevertheless very interesting that it shows up in the behaviour of the surface tension. Another striking feature of the result is the independence of the QGP droplet surface tension  $\sigma$  to variations in the flow parameters of the model and it varies with only the critical temperature, in the lowest order approximation we have employed.

The constancy of the ratio  $\sigma/T_c^3$  indicates a cubic critical temperature dependence of the surface tension of the interfacial separation between the two phases. This is in striking conformity with the results of lattice QCD simulations [12]. It is also heartening to note that for  $T_c \sim 156$  MeV,  $\sigma^{1/3} \sim 67$  MeV in our model which is exactly the value estimated in a MIT bag model calculation [13].

The graphs (figures 3–6) clearly indicate that the model predicts a weakly first-order transition at a temperature in the range  $(160 \pm 5)$  MeV, which seems to be consistent with current expectations of QGP–hadron phase transition [1]. The phase transition has to be characterised as weakly first-order as the discontinuities occurring in the first-order thermodynamic quantities are just about one standard deviation from the values of the quantities on the ordinates, namely the entropy  $S$  in figures 3 and 4.

The independence of the velocity of sound in the QGP system (figures 7 and 8), from both the values of the model flow parameters as well as the magnitude of the transition temperature is remarkable. The value of the velocity of sound is

consistently predicted to be of the order of  $(0.27 \pm 0.02)$  times the velocity of light in vacuum. The value for the velocity is in excellent agreement with recent model calculations [14], as well as with lattice simulations that include dynamical quarks [15], but as should be expected, it is at variance with pure gauge lattice results [16].

## References

- [1] H Satz, CERN-TH-2590, 18pp (1978)  
F Karsch, E Laermann, A Peikert, Ch Schmidt and S Stickan, *Nucl. Phys.* **B94**, 411 (2001)  
F Karsch and H Satz, *Nucl. Phys.* **A702**, 1 (2002)
- [2] T Renk, R Schneider and W Weise, *Phys. Rev.* **C66**, 014902 (2002)  
E Laermann and O Philipsen, *Ann. Rev. Nucl. Part. Sci.* **53**, 163 (2003)  
F Karsch and E Laermann, *Quark-gluon plasma III* edited by R Hwa, hep-lat/0305025
- [3] L P Csernai, J I Kapusta and E Osnes, *Phys. Rev.* **D67**, 045003 (2003)  
J I Kapusta, R Venugopalan and A P Vischer, *Phys. Rev.* **C51**, 901 (1995)  
L P Csernai and J I Kapusta, *Phys. Rev.* **D46**, 1379 (1992)  
L P Csernai and J Kapusta, *Phys. Rev. Lett.* **69**, 737 (1992)  
L P Csernai, J Kapusta, Gy Kluge and E E Zabrodin, *Z. Phys.* **C58**, 453 (1993)
- [4] R Ramanathan, Y K Mathur, K K Gupta and Agam K Jha, *Phys. Rev.* **C70**, 027903 (2004)  
R Ramanathan, Agam K Jha, K K Gupta and S S Singh, e-Print, hep-ph-0510196 (2005)
- [5] B D Malhotra and R Ramanathan, *Phys. Lett.* **A108**, 153 (1985); see also ref. [3]
- [6] A D Linde, *Nucl. Phys.* **B216**, 421 (1983)  
E Fermi, *Zeit F. Phys.* **48**, 73 (1928)  
L H Thomas, *Proc. Camb. Phil. Soc.* **23**, 542 (1927)  
H A Bethe, *Rev. Mod. Phys.* **9**, 69 (1937)
- [7] A Peshier, B Kampfer, O P Pavlenko and G Soff, *Phys. Lett.* **B337**, 235 (1994)  
V Goloviznin and H Satz, *Z. Phys.* **C57**, 671 (1993)
- [8] J L Richardson, *Phys. Lett.* **B82**, 272 (1979)
- [9] R Balian and C Bloch, *Ann. Phys.(NY)* **60**, 401 (1970)  
I Mardor and B Svetitsky, *Phys. Rev.* **D44**, 878 (1991)  
G Neerguard and J Madsen, *Phys. Rev.* **D60**, 054011 (1999)  
M G Mustafa, D K Srivastava and B Sinha, *Euro. Phys. J.* **C5**, 711 (1998)
- [10] H Weyl, *Nachr. Akad. Wiss Göttingen* (1911) p. 110
- [11] J Solfrank, P Huovinen, M Kataja, P V Ruuskanen, M Prakash and R Venugopalan, *Phys. Rev.* **C55**, 392 (1997)  
C M Hung and E Shuryak, *Phys. Rev.* **C57**, 1891 (1998)  
E Shuryak, *Prog. Part. Nucl. Phys.* **53**, 273 (2004)
- [12] Y Iwasaki, K Kanaya, Leo Karkkainen, K Rummukainen and T Yoshie, *Phys. Rev.* **D49(7)**, 3540 (1994)
- [13] L Paria, M G Mustafa and A Abbas, *Int. J. Mod. Phys.* **E9**, 149 (2000)
- [14] Sanjay K Ghosh, Tamal K Mukherjee, Munshi G Mustafa and Rajarshi Ray, *Phys. Rev.* **D73**, 114007 (2006)
- [15] A Ali Khan *et al*, *Phys. Rev.* **D64**, 074510 (2001)  
Yasumichi Aoki, Zoltan Fodor, Sandor D Katz and Kalman K Szabo, *J. High Energy Phys.* **01**, 089 (2006)
- [16] Rajiv V Gavai, Sourendu Gupta and Swagato Mukherjee, hep-lat/0506015